

Detection of Temperature Contours on the Thermal Distribution Generated by Ablation Micro-coaxial Antennas

Texar Javier Ramírez Guzmán
Department of Electrical
Engineering/Bioelectronics
CINVESTAV-IPN
México City, México.
texar.ramirezg@cinvestav.mx

Arturo Vera Hernández
Department of Electrical
Engineering/Bioelectronics
CINVESTAV-IPN
México City, México.
arvera@cinvestav.mx

Lorenzo Leija Salas
Department of Electrical
Engineering/Bioelectronics
CINVESTAV-IPN
México City, México.
lleija@cinvestav.mx

Citlalli Jessica Trujillo Romero
National Institute of Rehabilitation,
Division of Research
in Medical Engineering
México City, México.
cjtrujillo@inr.mx

Abstract — In order to improve the treatment planning of microwave ablation treatments, the temperature distribution must be known. Different designs of micro-coaxial antennas to treat bone tumors have been developed in order to modify the shape of the tissue damage. To evaluate the temperature distribution (generated by a micro-coaxial antenna), a novel way to acquire the contour of the temperature distribution obtained by thermal images was implemented. Four micro-coaxial antennas were evaluated in multilayer phantoms with an input power of 5 W applied per 5 minutes. Thermal images of the generated temperature distributions were obtained. To facilitate the detection of variations in the intensities of each pixel, the thermal images were processed in the intensity channel. Sobel operators were implemented in order to obtain a better contrast between the generating contour and the background of the images. The proposed algorithm allowed to obtain the contours of the temperature distribution generated by the antennas reaching temperatures above 60°C.

Keywords — microwave ablation, thermal images, temperature distribution, thermal image processing.

I. INTRODUCTION

As an alternative to clinical cancer treatments, minimally invasive heat treatments has been investigated [1]. Thermal ablation is defined as the direct application of heat to the tumor to cause its destruction [2]. To produce real therapeutic results, temperatures between 60°C-100°C must be achieved. In microwave ablation (MWA), a fine needle that works as an antenna is inserted inside the tumor to apply electromagnetic energy at microwave frequencies, usually 915 MHz or 2.45 GHz [3]. Although different types of MWA antennas have been proposed, the most common ones are the interstitial coaxial antennas. Recent improvements in antenna design, such as the ability to deliver a greater amount of electromagnetic energy to a more specific location and the generation of less heat in the rest of the antenna have been reported [4], [5], [6]. These studies show that MWA antennas are more suitable for treating different types of tumors.

One of the main problems during MWA treatments is related to the inability to know the contour of the temperature

distribution generated by the micro-coaxial antenna. Each antenna can generate different temperature distributions; moreover, it depends of the treatment time. Therefore, if the contour of the temperature distribution of the antenna can be known, the reliability of MWA treatment planning can be significantly improved. H. Gao *et al.* proposed a mapping method to obtain the thermal coagulation zones based on the results of FEM simulation [7]; however, the use of a thermal camera during MWA treatments allows obtaining an RGB image of the temperature distribution in the tissue surface [8] and does not to depend of the FEM simulation results. Despite this, the resulting thermal image is not enough to visualize the difference between antennas.

Edge detection filters allow locating areas where sharp intensity transitions occur. This type of filters can be used as tools to identify zones and borders between different intensities of a study area [9]. The image that has better spectral information is RGB mode. This mode involves three bands that corresponds to the colors red, green and blue. The RGB mode is only one of many ways to encode a color; this mode is the most frequent to register images and its representation on a screen, but it is not the only one. At the time of an image fusion, the use of other formats is more advantageous. One of the modes that can be used for this purpose is known as IHS [10]. The IHS panchromatic refining method converts the multispectral image from RGB to intensity (I), hue (H), and saturation (S). Low resolution intensity is replaced by high resolution panchromatic image. Edge detection is an important element for artificial vision, such as image processing and pattern recognition. The extraction of edges is based in the extraction of pixels with high variation in the intensity scale found in the image to be processed. This variations in the intensity for extraction of edges, contour or corners can be realized with different algorithms [11]. Sobel Edge detection is a widely used algorithm of edge detection in image processing. Along with Canny and Prewitt, Sobel is one of the most popular edge detection algorithms used in today's technology.

The main goal of this work is the development of an algorithm to obtain the contour of the temperature distribution

generated by micro-coaxial antennas using thermal images as a visual aid to understand how biological tissue is damaged during MWA procedures.

II. METHODOLOGY

A. Acquisition of thermal images

Four micro-coaxial antennas, metal-tip monopole antenna (MTM), metal-tip monopole choke antenna (MTM-C), double slot antenna (DS) and double slot choke antenna (DS-C), previously studied and optimized to be in contact with bone tissue were used to generate thermal ablation in multilayer phantoms [12]. These phantoms emulate a layer of fat, muscle and bone tissue in which the antenna was inserted. The antenna was fed with 5 W applied per 5 minutes. The radiation system to feed the antenna consisted in a power amplifier SSPA Aethercomm and a microwave generator Rohde & Schwarz SML03 with a work frequency of 2.45 GHz. The thermographic camera used to acquire the thermal images was a Fluke Ti32. The Table I shows the specifications of the camera. The camera was positioned at 50 cm of the phantom. A thermal image was captured every minute during the experiments obtaining a total of 5 images by each antenna. Figure 1 shows the experimental configuration to obtain the thermal images.

B. Image processing

Image enhancement methods can be applied to color (RGB) images by modifying the luminance component. It is commonly done in the IHS color space, which decorrelates the luminance channel of the color channels. Image enhancement is applied in intensity channel I, without processing channels H and S [13]. The channel I of an image is obtained as shown in Equation 1:

$$I = \frac{1}{3 \cdot 255} (R + G + B) \quad (1)$$

where R, G and B are the RGB channels of the thermal image and I is the intensity image obtained. To avoid the presence of irrelevant details in image I, as white or black pixels due to transmission errors or storage, a smoothing filter was used to reduce the noise. A Gaussian filter, which is an isotropic filter, was used. The response of this filter is independent of the orientation of the image. This filter produces a more uniform smoothing compared to other smoothing filters, such as the median filter. The Equation 2 shows the convolution between the Gaussian filter and the intensity image.

$$f_s(x, y) = G(x, y) * f(x, y) \quad (2)$$

where $G(x, y)$ is a 5x5 convolution kernel and $f(x, y)$ is the image I.

TABLE I
SPECIFICATIONS OF THE THERMOGRAPHIC CAMERA FLUKE TI32

Parameter	Value
Temperature range	-20°C to +600°C
Precision	±2°C
Thermal sensibility (NETD)	0.045°C and 45 mK
Total of pixels	76.800
Minimum focal distance	46 cm

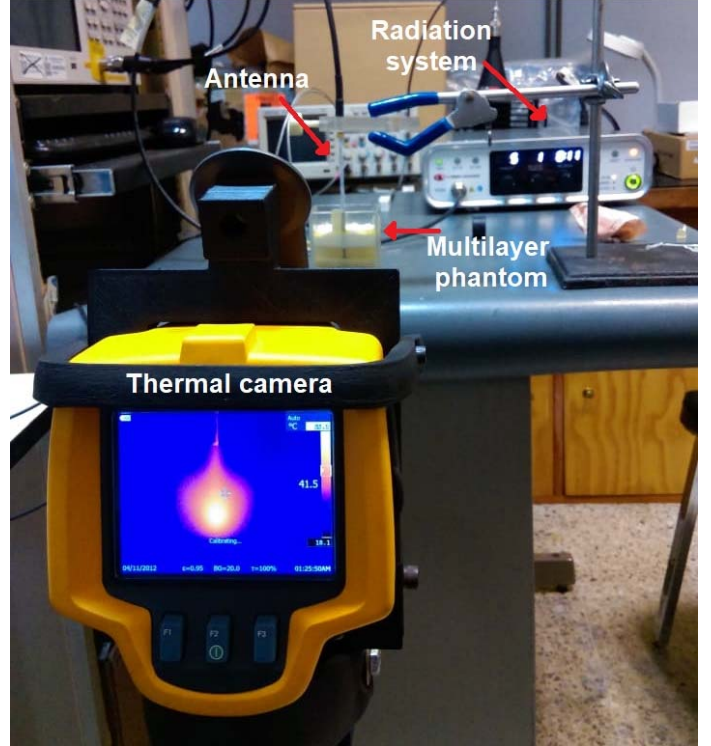


Figure 1. Experimental configuration to obtain the thermal images in microwave ablations by using interstitial antennas.

At this point, the $f_s(x, y)$ image shows the contour generated by the antenna. However, due to the use of the Gaussian filter for noise removal, the image $f_s(x, y)$ lose definition to the details. To apply a threshold on the $f_s(x, y)$ image to obtain a black and white mask of the contour image is inefficient. Therefore, the intensity gradient of the image was calculated to obtain an image with a more defined contour.

To obtain the intensity gradient of the image $f_s(x, y)$, the Sobel operators were used. The image $f_s(x, y)$ was filtered again by using a Sobel kernel as shown in Equation 3:

$$h_x = \begin{bmatrix} -1 & 0 & 1 \\ -2 & 0 & 2 \\ -1 & 0 & 1 \end{bmatrix} \text{ and } h_y = \begin{bmatrix} -1 & -2 & -1 \\ 0 & 0 & 0 \\ 1 & 2 & 1 \end{bmatrix}$$

thus

$$g_x = h_x * f_s(x, y) \text{ and } g_y = h_y * f_s(x, y) \quad (3)$$

where g_x and g_y is the intensity gradient in the horizontal and vertical direction, respectively. From g_x and g_y , the intensity gradient was calculated as shown in Equation 4:

$$|\nabla f_s(x, y)| = \sqrt{g_x(x, y)^2 + g_y(x, y)^2} \quad (4)$$

as a result, a sum of the coefficients equal to zero was obtained, so that, a response of zero was generated in regions of constant intensity. This obtained image was used to make a sum between the image $f_s(x, y)$ and the intensity gradient $|\nabla f_s(x, y)|$. The goal of making this sum is to obtain an image where the pixels that are part of the contour present similar intensity values. Then, a threshold will be applied on the image generated to obtain a mask of the contour obtained in black and white. This mask will be applied to the original thermal image. The sum is shown in Equation 5:

$$f_o(x, y) = |\nabla f_s(x, y)| + f_s(x, y) \quad (5)$$

where $f_o(x, y)$ is the image in which the threshold will be applied to obtain the black and white contour mask. The image $f_o(x, y)$ shows the contour of the temperature distribution with low intensity values (close to 0). To perform the threshold and obtain the mask of the contour in black and white, the minimum intensity value of the image that correspond to the contour generated by the antenna was searched and saved in a variable x . This minimum intensity value can be equal to a single contour pixel. For that reason, a constant c was added to have a pixel interval that corresponds to all the contour pixels, $x+c$. If the pixel of the image $f_o(x, y)$ is lower than $x+c$, it corresponds to the contour and it takes a value equal to zero. However, if it doesn't correspond to the contour, it takes a value equal to 1 corresponding to the background of the mask.

III. RESULTS

A. Thermal images

Figure 2 shows the thermal images generated by each antenna. The thermal images were obtained after 5 minutes of radiation with 5 W as input power. These thermal images were analyzed with the image processing proposed.

B. Image processing

The main objective of the image processing was to generate a black and white mask of the contour of the temperature distribution. This provides a visual context in the study of the micro-coaxial antennas behavior. Figure 3 shows the image processing step by step to get the mask of the thermal image.

Figure 3a shows that, with the extraction of the intensity channel of the thermal image, the contour of the temperature distribution becomes visible. Figure 3b is the result of applying the Gaussian filter for noise reduction in the image, it is observed

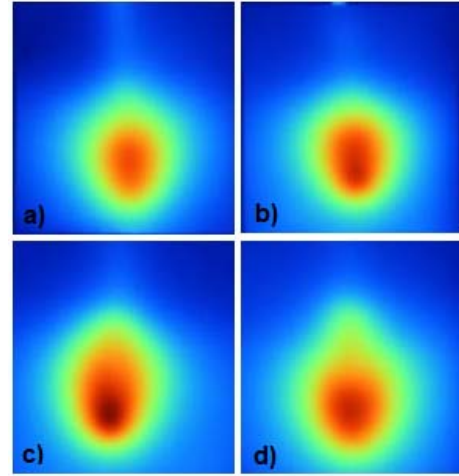


Figure 2. Thermal images obtained with a thermographic camera Fluke Ti32. a) MTM antenna, b) MTM-C antenna, c) DS antenna and d) DS-C antenna.

that the image loses definition to the details. In the Figure 3c, it is observed the intensity gradient generated by using the Sobel operators. Figure 3d shows the result of the sum of image 3b and 3c, to highlight the generated contour. Figure 3e shows the black and white mask obtained after the application of the threshold on the figure 3d. Figure 3f shows the temperature contour generated by the MTM antenna. Figure 4 shows a comparison between the contour of the temperature distribution using the proposed algorithm (Figure 4b) and the Canny method (Figure 4c). However, the contour presents some missing black pixel, *i. e.* the contour was incomplete, this was due to the variable $x+c$ used to do the threshold. If the variable $x+c$ is a number closer to the minimum intensity in the contour, the mask will present a smaller number of black pixels. Figure 5 shows the contour of the MTM antenna by using different values in the variable $x+c$. Based on the results observed in Figure 5, a constant c equal to 40 was considered to carry out the processing of the thermal images of the four antennas. Figure 6 shows the results of the processing of the four thermal images generated by each antenna.

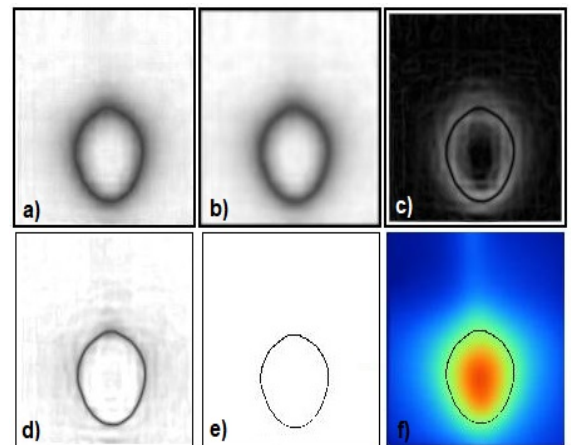


Figure 3. Processing of the thermal image of an MTM antenna. a) channel I of the thermal image, b) channel I filtered with the Gaussian filter, c) intensity gradient, d) result of the sum between image 3b and 3c, e) black and white mask and f) positioning of the mask on the original thermal image.

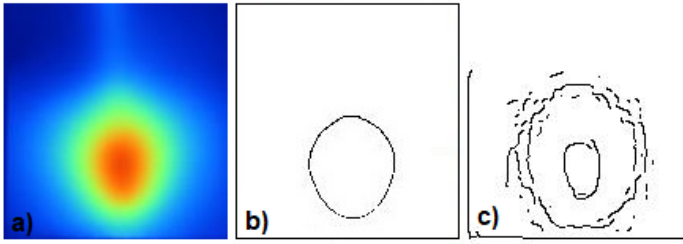


Figure 4. Contour of the temperature distribution of an MTM antenna. a) thermal image, b) proposed algorithm and c) edge detection using Canny method.

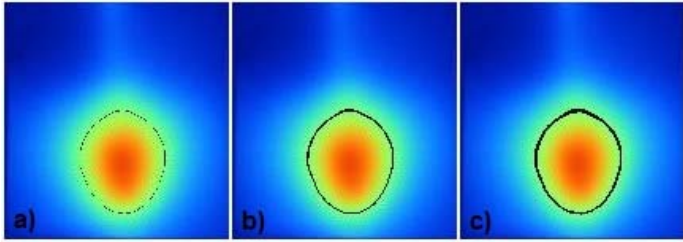


Figure 5. Effects of the use different values for the variable $x+c$. a) constant $c=15$, b) constant $c=40$ and c) constant $c=60$.

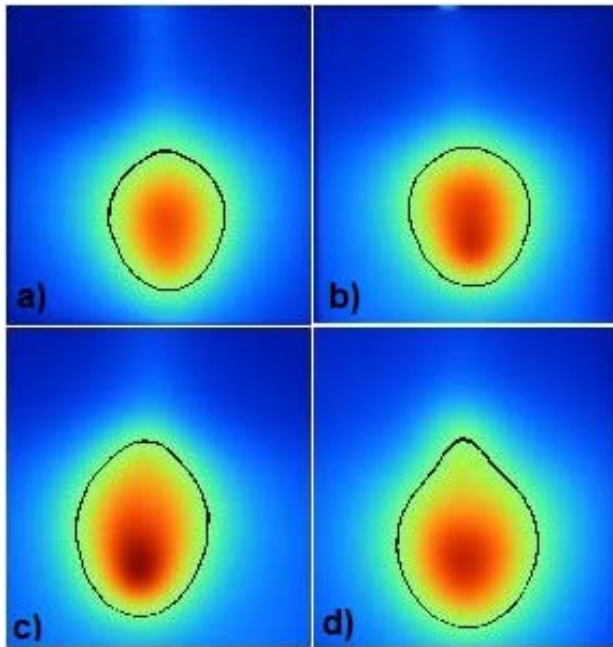


Figure 6. Contour of the temperature distribution generated by micro-coaxial antennas. a) MTM antenna, b) MTM-C antenna, c) DS antenna and d) DS-C antenna.

IV. DISCUSSION

This work is a first approach to detect the areas that reached the ablation temperatures generated by the antennas and to know the amount of damaged tissue. To obtain the contour that limited the tissue under ablation temperatures will facilitate the calculation of the damaged tissue during clinical applications. The precise evaluation of how tissue is damaged during MWA treatments plays a very important role in the obtain of successful

results. To know the temperature distribution is important in order to have better treatment planning about the choice of the antenna to be used. According to this, the MTM and MTM-C antennas (See figure 6a and 6b) will have a better coupling with bone tumors that have a circular shape. The DS and DS-C antennas (See figure 6c and 6d) can be used to treat bone tumors with an elliptical shape.

In Figure 4 it is observed that, when using a conventional edge detection method such as the Canny method, irregular edges are obtained that do not correspond to the way in which the heat is distributed, so when using Sobel operators we can adapt the edge detection to a specific objective, in this case, the contour of the temperature distribution of the antennas. The processing of the thermal images must begin with the preparation and correction of these images to promote the good development of information extraction and improve the results obtained. The Gaussian filter allows to reduce image noise by convolving the image with a Gaussian filter kernel. The size of the kernel to use will depend on the amount of noise in the image. Thermal images generated by the antennas have a very low noise; therefore, a 5×5 size kernel was enough for image processing. If the amount of noise in the image is higher, a larger size kernel should be chosen. The threshold function performed to generate the contour mask is one of the most important steps in this algorithm. In Figure 3d, it is observed that the pixels that form the contour present similar intensity values. The minimum intensity value in the contour in the Figure 3d, just represent one pixel of the contour. For this reason, the threshold function ($x+c$) adds a constant c to the minimum intensity value (x) to find pixels with intensity values close to the variable x . The importance of detecting all the pixels that make up the contour of the temperature distribution will allow future work to calculate the area of damaged tissue.

V. CONCLUSION

This work was based on the processing of the thermal images obtained during experiments to analyze the behavior of different micro-coaxial antennas. This processing was carried out in the intensity channel of the thermal image without considering the temperatures reached during the experiments. The use of Sobel operators to generate the intensity of the gradient allowed a better thresholding of the processed image to generate a mask with the contour of the temperature, the proposed algorithm allowed to obtain the contours of the temperature distribution generated by the antennas reaching temperatures above 60°C . Future work will include contour detection based on the temperatures reached in the experiments to calculate the area of the damaged tissue.

ACKNOWLEDGMENT

We appreciate the funding for the development of the work presented project: ERAnet-EMHE 200022, CYTED-DITECROD-218RT0545 and Proyecto IV-8 call Amexcid-Auci 2018-2020.

REFERENCES

- [1] Q. Y. Fan *et al.*, “Microwave ablation of malignant extremity bone tumors,” *Springerplus*, vol. 5, no. 1, pp. 0–5, 2016.
- [2] T. B. West and T. S. Alster, “Percutaneous RF Interstitial Thermal Ablation in the Treatment of Hepatic Cancer,” no. September, pp. 759–768, 1996.
- [3] R. Ortega-Palacios, C. J. Trujillo-Romero, M. F. J. Cepeda-Rubio, L. Leija, and A. V. Hernández, “Heat transfer study in breast tumor phantom during microwave ablation: Modeling and experimental results for three different antennas,” *Electron.*, vol. 9, no. 3, 2020.
- [4] C. L. Brace, “Microwave Tissue Ablation: Biophysics, Technology and Applications,” *Crit Rev Biomed Eng*, vol. 38, no. 1, pp. 65–78, 2010.
- [5] C.J. Trujillo-Romero, G. Rico, L. Leija, A. Vera, J. Gutiérrez, “Micro-Coaxial Slot Antenna to Treat Bone Tumors by Thermal Ablation: Theoretical and Experimental Evaluation,” *IEEE Lat. Am. Trans*, 2018.
- [6] F. Lujan, B. Pinilla, J. Gutierrez-Martinez, A. Vera, L. Leija, C.J. Trujillo-Romero, “Theoretical Model of MWA Antennas to Treat Bone Tumors: One Slot and One Slot Choked Antennas.”
- [7] H. Gao, “Characterization of 2450-MHz microwave thermal coagulation zone based on characteristic length growth model and shape variation factor,” no. January, pp. 1–12, 2019.
- [8] T.J. Ramírez-Guzmán, C.J. Trujillo-Romero, A. Vera, L. Leija, “Micro-coaxial Monopole Antenna to Treat Bone Cancer: Design and Preliminary Experimentation,” *Glob. Med. Eng. Phys. Exch. Am. Heal. CARE Exch.*, 2019.
- [9] O. R. Vincent, Folorunso O. “A Descriptive Algorithm for Sobel Image Edge Detection,” *Proc. Informing Sci. IT Educ. Conf.*, 2009.
- [10] P.M. Mather, *Computer Processing of Remotely-sensed Images*. John Wiley & sons, 1999.
- [11] G. Pajares-Martinez, J. Cruz-Garcia, *Visión por computador imágenes digitales y aplicaciones*, 2da edición. .
- [12] T.J. Ramírez-Guzmán, A. Vera, L. Leija, C.J. Trujillo-Romero, “Antennas Design for Microwave Ablation in Bone Tissue : Simulation and Experimental Validation,” *Int. Conf. Electr. Eng. Comput. Sci. Autom. Control*, no. 1, pp. 3–7, 2019.
- [13] R. Gonzalez, R. Wood, *Digital Image Processing*, 3rd editio. .